Structure of Phase-Separated Ferroelectric/Semiconducting Polymer Blends for Organic Non-volatile Memories

McNeill, Christopher R.; Asadi, Kamal; Watts, Benjamin; Blom, Paul W. M.; de Leeuw, Dago M.

Published in:
Small

DOI:
10.1002/smll.200901719

Polymer blends

Structure of Phase-Separated Ferroelectric/Semiconducting Polymer Blends for Organic Non-volatile Memories**

Christopher R. McNeill, Kamal Asadi, Benjamin Watts, Paul W. M. Blom, and Dago M. de Leeuw*

Organic electronic devices such as transistors, light-emitting diodes, and solar cells are an attractive new technology that is seeking to benefit from the unique properties of organic materials such as flexibility and low-temperature solution processability to realize new applications.[1] Full organic electronic circuitry also requires the development of organic non-volatile memories with long retention time and high programming cycle endurance.[2] Insulating ferroelectric polymers such as the random copolymer poly(vinylidene fluoride-trifluoroethylene) (P(VDF-TrFE); 65:35; Figure 1a) are promising materials for use in organic non-volatile memories due to their ability to switch between two distinguishable polarizations through the application of an electric field. The simplest memory device based on polymers such as P(VDF-TrFE) is a ferroelectric capacitor where information is stored by aligning the direction of the internal polarization with an electric field. To retrieve information a switching voltage is applied to obtain either a high or low charge displacement current depending on the state of the internal polarization. As this read operation can affect the stored information, ferroelectric capacitors have a so-called destructive read-out[3] that severely hampers practical application. Recently, a breakthrough in the development of non-volatile organic memories was demonstrated by blending the ferroelectric polymer P(VDF-TrFE) with the semiconducting polymer, regio-random poly(3-hexylthiophene) (rir-P3HT; Figure 1a).[4] Non-volatile memory functionality was demonstrated in rir-P3HT:P(VDF-TrFE) blends based on resistive switching, with the polarization of the ferroelectric polymer modulating charge injection into the rir-P3HT phase and, hence, modulating the current flowing through the diode. It was tentatively proposed that the polarization field of the ferroelectric modulates the injection barrier at the metal-semiconductor contact.[4] This operation mechanism therefore relies upon the formation of phase-separated networks with a continuous phase of the minority rir-P3HT component between the top and bottom electrode.[4] Here we present the results of a X-ray microscopy study demonstrating the existence of a phase-separated, columnar morphology in rir-P3HT:P(VDF-TrFE) blends with rir-P3HT-rich domains of $\approx$100 to 500 nm surrounded by a continuous, essentially pure P(VDF-TrFE) phase.

Synchrotron-based scanning transmission X-ray spectromicroscopy (STXM) is a powerful tool for the study of the bulk morphology of thin-film polymer blends.[5] Contrast in STXM is provided by differences in the near-edge X-ray absorption fine structure (NEXAFS) spectra of the component materials and for organic materials with similar elemental composition; STXM typically utilizes differences in the carbon K-edge NEXAFS spectra of the constituent materials. Carbon K-edge NEXAFS spectra consist of peaks due to resonant transitions of electrons from the occupied 1s orbital to unoccupied π^* and σ^* states superimposed on an ionization step due to the excitation of 1s electrons to the ionization continuum. Thus contrast can be achieved with STXM due to differences in unoccupied electronic structure (i.e., differences in molecular antibonding orbitals), as well as differences in the elemental composition or electron density of the materials. Utilizing a transmission

[*] Dr. C. R. McNeill
Cavendish Laboratory, University of Cambridge
J J Thomson Ave, Cambridge, CB3 0HE (UK)
E-mail: crm51@cam.ac.uk
K. Asadi, Prof. P. W. M. Blom, Prof. D. M. de Leeuw
Zernike Institute for Advanced Materials, University of Groningen
Nijenborgh 4, NL-9747 AG, Groningen (The Netherlands)
Dr. B. Watts
Swiss Light Source, Paul Scherrer Institut
Villigen-PSI, CH-5232 (Switzerland)
Prof. P. W. M. Blom
Holst Centre
High Tech Campus 31
5605 KN Eindhoven (The Netherlands)
Prof. D. M. de Leeuw
Philips Research Laboratories, High Tech Campus 4
NL-5656 AE, Eindhoven (The Netherlands)

[**] The authors thank the ALS and SLS for beam-time, David Kilcoyne (ALS) and Jörg Raabe (SLS) for technical assistance, and Torben Schuettfort (U. Cambridge) for assistance with data acquisition. This work was supported by the Engineering and Physical Sciences Research Council, UK (Advanced Research Fellowship EP/E051804/1). The ALS is supported by the Director, Office of Science, Office of Basic Energy Sciences, of the USA Department of Energy under Contract DE-AC02-05CH11231. PolLux is funded by the BMBF (Project No. 05KS7WE1).

Supporting Information is available on the WWW under http://www.small-journal.com or from the author.

DOI: 10.1002/smll.200901719

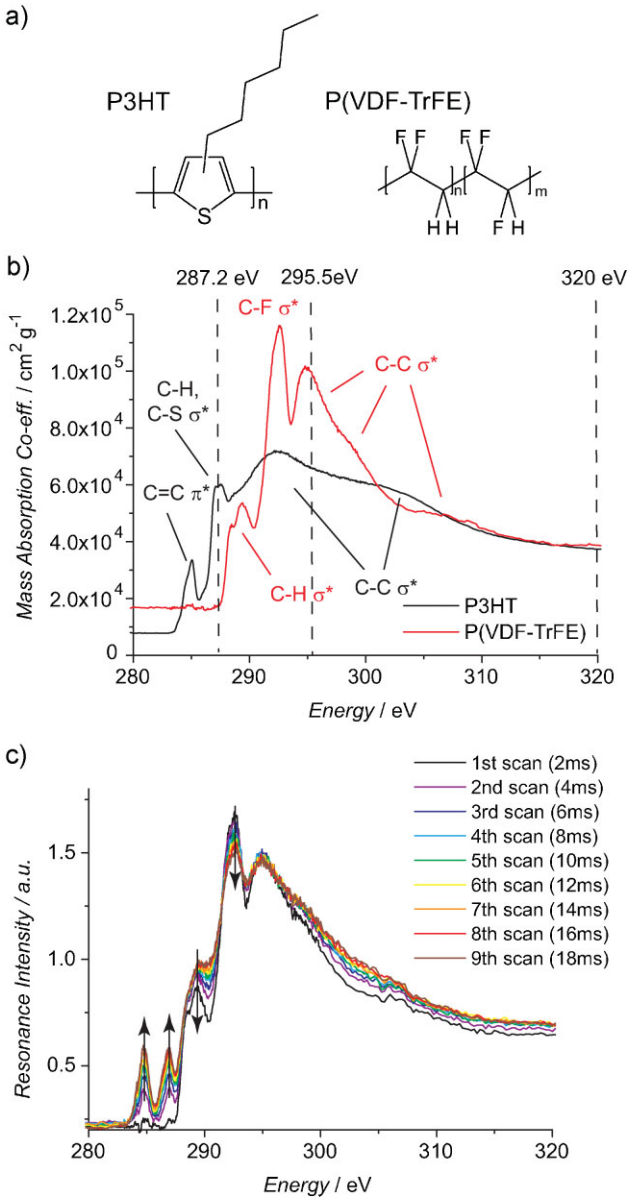

Figure 1. a) Chemical structures of rir-P3HT and P(VDF-TrFE). b) NEXAFS spectra of pristine films of rir-P3HT and P(VDF-TrFE). The major peaks are assigned to transitions from 1s to particular unoccupied orbitals and the three energies at which X-ray images were acquired are also shown. c) Evolution of radiation damage in the NEXAFS spectra of a P(VDF-TrFE) film. Spectra were taken by repeatedly scanning across the same 10-μm-long line with a dwell time of 2 ms per 50-nm linear region.

geometry, STXM is able to study films from a few to several hundred nanometers in thickness, and by acquiring images at different energies (or full NEXAFS spectra of selected regions), it is capable of providing quantitative chemical mapping of local blend composition. The X-ray beam is focused with the use of a zone plate to a spot-size (theoretical Rayleigh resolution) of 30 nm, thus combining high chemical sensitivity with excellent spatial resolution. STXM has previously been utilized to study insulating polymer blends such as polystyrene and poly(methyl methacrylate)[6] as well as to study the structure of conjugated polymer blends used in organic light-emitting diodes and solar cells.[7,8]

Figure 1 shows the bulk NEXAFS spectra of rir-P3HT and P(VDF-TrFE) taken of unblended reference samples. The mass absorption coefficient scale was determined using mass densities of 1.1 g cm^{-3} for rir-P3HT[9] and 1.9 g cm^{-3} for P(VDF-TrFE)[10] along with the thickness of the films. The NEXAS spectrum of rir-P3HT resembles that of region-regular P3HT with a 1s to $\pi^*_{C=C}$ peak at 285 eV, a 1s to $\sigma^*_{C-S/C-H}$ peak at 287.2 eV and higher lying 1s to σ^*_{C-C} peaks at 293 and 303 eV.[11] The NEXAFS spectrum of P(VDF-TrFE) is similar to previous observations, with no 1s to $\pi^*_{C=C}$ peak due to the lack of unsaturated C–C bonds.[12] The lowest lying peaks at 288.5 and 289.3 eV have been attributed to 1s to σ^*_{C-H} transitions, the peak at 292.6 eV to the 1s to σ^*_{C-F} resonance, and the higher lying peaks 295 eV and above to 1s to σ^*_{C-C} transitions.[12] While good contrast may be expected using an energy of 285 eV due to the lack of a 1s to $\pi^*_{C=C}$ resonance in P(VDF-TrFE), images were instead taken at 287.2 eV (P3HT-sensitive), 295.5 eV (P(VDF-TrFE)-sensitive), and 320 eV (chemically insensitive) due to issues associated with radiation damage in P(VDF-TrFE). In particular, repeated low dose line-scans of the same region (accumulating a high radiation dose) of a pure P(VDF-TrFE) film demonstrate that radiation damage causes a change in the P(VDF-TrFE) spectrum (Figure 1c) with a reduction in the intensity of the 1s to σ^*_{C-F} resonance and evolution of peaks at 285 and 286.7 eV. These two new peaks are likely to be due to the creation of unsaturated C–C π^* bonds due to an X-ray induced breaking of C–F bonds. Although clean reference spectra of P(VDF-TrFE) can be acquired by taking line-scans over a large area with a defocused beam to minimize radiation damage, imaging necessarily requires the use of a focused beam, making radiation damage unavoidable. The 1s to σ^*_{C-C} transition in P(VDF-TrFE), in contrast, is largely insensitive to radiation damage, as is the entire spectrum of rir-P3HT. Therefore, we have chosen the aforementioned energies for imaging as the influence of radiation damage at these energies is minor while maintaining good chemical contrast. In particular, at 287.2 eV the 1s to $\sigma^*_{C-S/C-H}$ peak in P3HT provides sensitivity to P3HT with only a minor contribution from radiation-damaged P(VDF-TrFE). The 295.5 eV, 1s to σ^*_{C-C} peak in P(VDF-TrFE) similarly provides preferential absorption by P(VDF-TrFE) without significant influence of radiation damage.

Figure 2 presents X-ray microscopy images of annealed and unannealed rir-P3HT:P(VDF-TrFE) blends with weight ratios of 10 and 1 wt% rir-P3HT. A rir-P3HT content of 10 wt% has been found to be optimum with both current density and on–off current modulation increasing with rir-P3HT content up to 10 wt% before decreasing.[13] This optimum blend content is believed to correspond to the situation where the rir-P3HT domain size is of the order of the charge-accumulation width. Thus, clear imaging of domain size as a function of rir-P3HT content is important for clarifying this relationship between weight ratio (and hence morphology) and memory switching. Annealing was performed at 140 °C for 2 h in a vacuum oven to enhance the crystallinity of the P(VDF-TrFE) phase. Also shown for comparison are atomic force microscope (AFM) images taken of the same films, albeit at different regions. The scale bar of the X-ray microscopy images is the X-ray optical density defined as $OD = \ln(I_0/I)$ where I is the measured X-ray

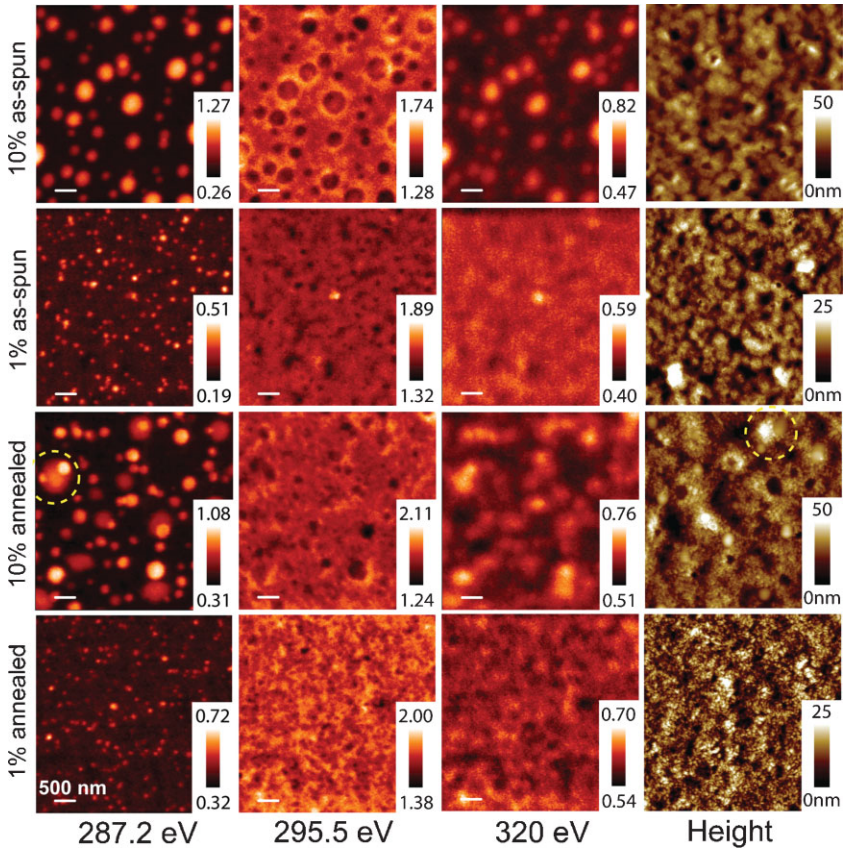

Figure 2. X-ray absorption images (first 3 columns) and AFM images (last column) of as-spun and annealed P3HT:P(VDF-TrFE) films with weight ratios of 10 and 1 wt% P3HT. All images are $5 \times 5\ \mu m^2$ and share a common scale bar.

intensity transmitted through the film and I_0 is the incident X-ray intensity. While the AFM images provide hints of an underlying phase-separated structure, the X-ray microscopy images clearly show a columnar, phase-separated morphology of P3HT-rich columns of lateral dimension 100 to 500 nm surrounded by an interconnected P(VDF-TrFE)-rich phase. For the unannealed 10 wt% P3HT film there is a clear correspondence between the 287.2 eV image and the 295.5 eV image, with the latter representing a negative image of the former. The 320 eV image at which there is little chemical contrast corresponds to an effective carbon density image, and shows less pronounced features than the 287.2 eV image, demonstrating the utility of X-ray spectromicroscopy to reveal internal, bulk chemical contrast. The 1 wt% P3HT film also shows a clear, phase-separated structure with columnar nature with feature size of ≈100 nm (see also cross-sectional traces in the Supporting Information, Figure S2). A cursory comparison of the as-spun and annealed films shows that the length-scale of lateral phase separation does not change significantly with annealing, however, there do appear to be some subtle changes in morphology that will be discussed below.

Examining the AFM images, raised or depressed circular features are seen (particularly in the 10 wt% rir-P3HT films) that correspond roughly to the size of the rir-P3HT-rich phase observed with X-ray microscopy (see also phase images in the Supporting Information, Figure S3). A pronounced increase in the roughness of the P(VDF-TrFE) phase is seen with annealing, consistent with the crystallization of this phase, confirmed by X-ray diffraction measurements.[13] Scanning electron microscopy images taken of the top of annealed films also show smooth, circular regions surrounded by a rough, needle-like phase[13] consistent with the identification of the circular features observed in AFM as the top of the bulk, columnar P3HT-rich phases. Furthermore, the areal density of the circular features observed with AFM is similar to the density of P3HT-rich phases observed with STXM, demonstrating that the bulk, columnar phases observed by STXM in general continue through to the top surface of the film.

While the length scale of phase separation does not change significantly with annealing, there are some subtle differences in the shape of the rir-P3HT domains before and after annealing. In particular, in the 287.2 eV annealed 10 wt% P3HT image, a number of larger domains show additional structure in the form of brighter, secondary phases with smaller diameter (example highlighted). A similar feature is observed in the AFM image of this film (also highlighted), consisting of a rough, raised circular feature with two smaller smooth features at the edge. Furthermore, comparison of the 287.2 and 295.5 eV images of the annealed 10 wt% film shows a less-clear correspondence than observed for the unannealed 10 wt% 287.2 and 295.5 eV images (also observed in other images taken of 10 wt% films and also in films of 5 and 2 wt% rir-P3HT; see Supporting Information, Figure S1). These observations suggest the lateral overgrowth of some of the P3HT phases by the needle-like P(VDF-TrFE) phase at the surface with annealing. Connectivity to the underlying P3HT phase, however, is maintained through the smaller sub-phases that penetrate the surface. Of course, one has to be careful of reading too much vertical information from the STXM images. In explaining the subtle changes in bulk morphology with annealing one would also need to consider the presence of a wetting layer at the substrate/film interface that has been observed in other laterally phase-separated polymer blend systems.[14] However, these results do suggest an additional vertical structure in these films that should be investigated further with surface-sensitive techniques.

The local blend composition has also been investigated quantitatively by acquiring full NEXAFS spectra at selected regions of an unannealed 10 wt% rir-P3HT film. Due to the problem of radiation damage as discussed above, spectra were acquired of four separate regions with a slightly defocused beam and low dwell times in order to minimize radiation damage that were then averaged to acquire spectra with acceptable statistics. Figure 3 displays the NEXAFS spectra taken of rir-P3HT-rich and P(VDF-TrFE)-rich regions taken in

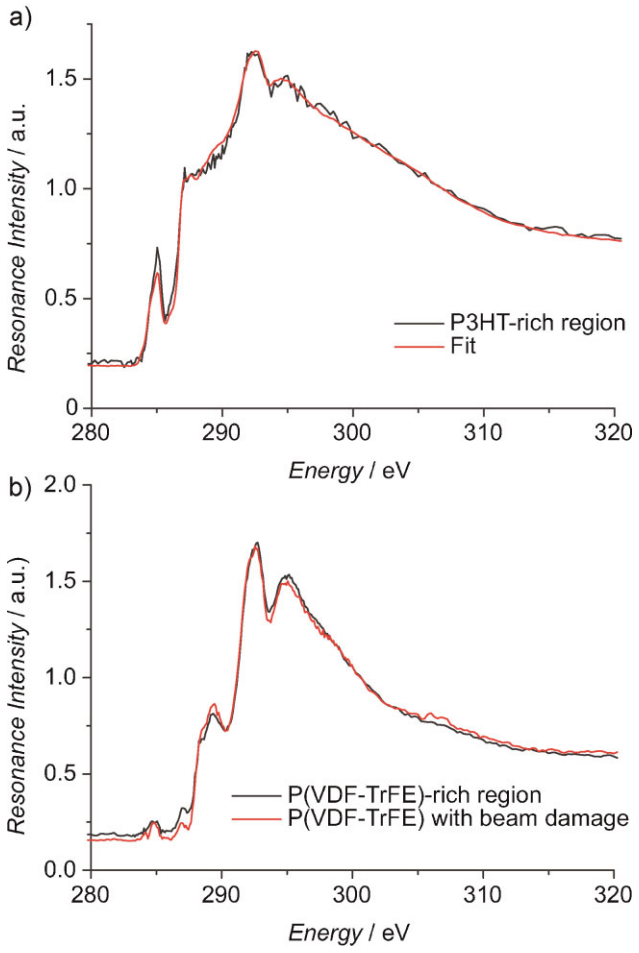

Figure 3. a) Averaged NEXAFS spectrum of P3HT-rich regions (black) in an unannealed P3HT:P(VDF-TrFE) blend with 10 wt% P3HT. Also shown is a fit to the data (red) with a linear combination of pristine P3HT and P(VDF-TrFE) NEXAFS spectra giving a local blend ratio of 78 wt% P3HT. b) Averaged NEXAFS spectrum of P(VDF-TrFE)-rich regions in an unannealed P3HT:P(VDF-TrFE) blend (black) with 10 wt% P3HT. Shown for comparison is the spectrum of an unblended P(VDF-TrFE) (red).

this manner. Also displayed are fits to these blend spectra with a linear combination of unblended rir-P3HT and P(VDF-TrFE) spectra. For the case of the P3HT-rich region, a significant component of P(VDF-TrFE) (22 wt%) is required to provide a good fit to the blend spectrum. The presence of P(VDF-TrFE) in the rir-P3HT-rich region may be due to bulk intermixing of P(VDF-TrFE) in the rir-P3HT phase, or due to the presence of additional vertical structure as discussed above. The spectrum of the P(VDF-TrFE)-rich region closely resembles that of pure P(VDF-TrFE). Comparison of this spectrum to that of a pure P(VDF-TrFE) film with mild radiation damage indicates that the P(VDF-TrFE)-rich region can be regarded as being essentially pure to within experimental limits (≈1 wt%).

In summary, we have revealed the internal, phase-separated structure of rir-P3HT:P(VDF-TrFE) films used in non-volatile organic memories. The morphology of these films is characterized by a phase-separated, columnar morphology with rir-P3HT-rich domains of purity ≥80 wt% and size ≈100 to 500 nm surrounded by a continuous, essentially pure P(VDF-TrFE) phase. Comparison of AFM (surface) and STXM (bulk) images reveal a similar areal density of P3HT-rich phases, indicating good connectivity of the bulk phases to the surface. These observations confirm the previous hypothesis of a phase-separated structure in these films that is necessary for their operation as resistive switches with transport through the rir-P3HT phase with injection of charge to the rir-P3HT phase modulated by the polarization field of P(VDF-TrFE) phase. The STXM data also suggest the presence of an additional vertical morphology that is influenced by annealing and will be investigated in future studies.

Experimental Section

Sample preparation: The ferroelectric polymer P(VDF-TrFE) (65:35) was purchased from Solvay and used without further purification. Rir-P3HT was purchased from Rieke Metals and purified by dissolving in distilled toluene, dedoping with hydrazine, and precipitating in methanol. The fraction collected was Soxhlet-extracted with methanol, n-hexane, and dichloromethane until the extraction solvent was colorless. The dichloromethane fraction was precipitated in methanol, collected, dissolved in chloroform, and precipitated again in methanol. This collected high-molecular-weight rir-P3HT fraction was dried under vacuum and stored in a glove box under nitrogen atmosphere. Blends of rir-P3HT:P(VDF-TrFE) were prepared with different weight ratios of 1, 2, 5, and 10 wt% rir-P3HT. Tetrahydrofuran (THF) was used to co-dissolve the materials with a total concentration of 30 mg mL^{-1}. For reference samples, pure rir-P3HT (5 mg mL^{-1}) and P(VDF-TrFE) (30 mg mL^{-1}) were prepared in toluene and THF, respectively. Solutions were filtered with 1-μm poly(tetrafluoroethylene) (PTFE) filters. Films were either spin-coated onto glass or poly(3,4-ethylenedioxythiophene):poly(styrene sulfonic acid) (PEDOT:PSS)-coated glass (70 nm, H. G. Starck) to aid the float-off of annealed samples. The PEDOT:PSS layer was dried in an oven at 140 °C for 10 min prior to blend deposition. Blend films were spin-coated in a nitrogen-filled glove box onto glass (for the case of unannealed films) or PEDOT:PSS-coated glass (for annealed films) with film thickness in the range of 120–200 nm. Annealed blends were annealed at 140 °C in a vacuum oven for 2 h with slow heating and cooling rates. For X-ray microscopy investigation films were floated off onto deionized water and picked up with transmission electron microscopy (TEM) grids. Annealed rir-P3HT:P(VDF-TrFE) films became too strongly adhered to the glass substrate, hence the need of a sacrificial, water-soluble PEDOT:PSS layer. Identical morphologies were observed by AFM for films processed on glass and PEDOT:PSS and by STXM for unannealed films processed on glass and PEDOT:PSS-coated glass.

Surface metrology: Surface topography was characterized with a Digital Instruments Nanoscope IIIa AFM in tapping mode. AFM images were performed on the same films that were investigated with X-ray microscopy. Film thickness was determined with a Dektak 6M profilometer.

X-ray microscopy: NEXAFS spectromicroscopy was performed at beamline 5.3.2 at the Advanced Light Source, Berkeley, California[15,16] and at the PolLux beamline at the Swiss Light Source, Paul Scherrer Institut, Villigen, Switzerland.[17,18] TEM grid-supported films were mounted in the sample chamber, which

was either evacuated to low vacuum (SLS) or evacuated to low vacuum and subsequently refilled with 1/3 atm of helium (ALS). The transmitted X-ray intensity through the film was recorded using a scintillator and photo-multiplier tube and measured as a function of energy (280.0 to 320.0 eV with a resolution of 0.1 eV) and position (with resolution better than 40 nm.) Transmitted X-ray intensity was converted to a X-ray optical density by recording the X-ray intensity through a region of the TEM grid with no film. X-ray images were taken at 280 (pre-edge, not shown), 287.2, 295.5, and 320 eV. For quantitative determination of local composition, full NEXAFS spectra (typically 259 points between 278 and 320 eV with 0.1 eV resolution between 283 and 298 eV) were taken over selected linear regions of the blend with a slightly defocused beam and dwell time of 0.5 ms to minimize radiation damage. Reference spectra of unblended rir-P3HT and P(VDF-TrFE) films were taken over 20 μm with a defocused beam and dwell time of 5 ms. Fitting of blend spectra was done using the conjugate gradient optimization fitting routine in aXis2000.[19] Further experimental and analysis details can be found in a previous communication.[7]

Keywords:
non-volatile memories · organic electronics · polymer blends · semiconductors

[1] S. R. Forrest, *Nature* **2004**, *428*, 911.
[2] J. C. Scott, L. D. Bozano, *Adv. Mater.* **2007**, *19*, 1452.
[3] J. F. Scott, *Ferroelectric Memories*, Springer, Heidelberg **2000**.
[4] K. Asadi, D. M. De Leeuw, B. De Boer, P. W. M. Blom, *Nat. Mater.* **2008**, *7*, 547.
[5] H. Ade, H. Stoll, *Nat. Mater.* **2009**, *8*, 281.
[6] C. Morin, H. Ikeura-Sekiguchi, T. Tyliszczak, R. Cornelius, J. L. Brash, A. P. Hitchcock, A. Scholl, F. Nolting, G. Appel, D. A. Winesett, k. Kaznacheyev, H. Ade, *J. Electron Spectrosc. Relat. Phenom.* **2001**, *121*, 203.
[7] C. R. McNeill, B. Watts, L. Thomsen, W. J. Belcher, N. C. Greenham, P. C. Dastoor, *Nano Lett.* **2006**, *6*, 1202.
[8] C. R. McNeill, B. Watts, L. Thomsen, W. J. Belcher, A. K. D. Kilcoyne, N. C. Greenham, P. C. Dastoor, *Small* **2006**, *2*, 1432.
[9] T. J. Prosa, M. J. Winokur, J. Moulton, P. Smith, A. J. Heeger, *Macromolecules* **1992**, *25*, 4364.
[10] T. R. Dargaville, M. Celina, J. W. Martin, B. A. Banks, *J. Polym. Sci, Part B: Polym. Phys.* **2005**, *43*, 2503.
[11] D. M. DeLongchamp, B. M. Vogel, Y. Jung, M. C. Gurau, C. A. Richter, O. A. Kirillov, J. Obrzut, D. A. Fischer, S. Sambasivan, L. J. Richter, E. K. Lin, *Chem. Mater.* **2005**, *17*, 5610.
[12] D. Schmeisser, M. Tallarida, K. Henkel, K. Müller, D. Mandal, D. Chumakov, E. Zschech, *Mater. Sci.-Pol.* **2009**, *27*, 141.
[13] K. Asadi, H. J. Wondergem, C. R. McNeill, N. Singelin, P. W. M. Blom, D. M. de Leeuw, unpublished.
[14] A. M. Higgins, S. J. Martin, R. J. Thompson, J. Chappell, M. Voigt, D. G. Lidzey, R. A. L. Jones, M. Geoghegan, *J. Phys.: Condens. Matter* **2005**, *17*, 1319.
[15] A. L. D. Kilcoyne, T. Tyliszczak, W. F. Steele, F. S, P. Hitchcock, K. Franck, E. H. Anderson, B. D. Harteneck, E. G. Rightor, G. E. Mitchell, A. P. Hitchcock, L. Yang, T. Warwick, H. Ade, *J. Synchrotron Radiat.* **2003**, *10*, 125.
[16] T. Warwick, H. Ade, D. Kilcoyne, M. Kritscher, T. Tyliszczak, S. Fakra, A. Hitchcock, P. Hitchcock, H. Padmore, *J. Synchrotron Radiat.* **2002**, *9*, 254.
[17] U. Flechsig, C. Quitmann, J. Raabe, M. Booge, R. Fink, H. Ade, presented at *9th International Conference on Synchrotron Radiation Instrumentation (SRI 2006)*, Daegu, South Korea, May 28–June 02, 2006.
[18] J. Raabe, G. Tzvetkov, U. Flechsig, M. Boge, A. Jaggi, B. Sarafimov, M. G. C. Vernooij, T. Huthwelker, H. Ade, D. Kilcoyne, T. Tyliszczak, R. H. Fink, C. Quitmann, *Rev. Sci. Instrum.* **2008**, *79*, 10.
[19] Homepage of aXis2000 software developed by Adam P. Hitchcock, http://unicorn.mcmaster.ca/aXis2000.html (accessed March 2009).

Received: September 14, 2009
Revised: November 25, 2009
Published online: January 27, 2010

